Journal of Microbiological Methods 165 (2019) 105692

Contents lists available at ScienceDirect

Journal of Microbiological Methods

journal homepage: www.elsevier.com/locate/jmicmeth

Eco-friendly synthesis of silver nanoparticles using *Senna alata* bark extract and its antimicrobial mechanism through enhancement of bacterial membrane degradation

Julalak C. Ontong[a], Supakit Paosen[a,b], Shiv Shankar[c,*], Supayang P. Voravuthikunchai[a,b,**]

[a] Natural Product Research Center of Excellence, Prince of Songkla University, Hat Yai, Songkhla 90112, Thailand
[b] Department of Microbiology, Faculty of Science and Excellence Research Laboratory on Natural Products, Prince of Songkla University, Hat Yai, Songkhla 90112, Thailand
[c] Center for Humanities and Sciences, BioNanocomposite Research Center, Department of Food and Nutrition, Kyung Hee University, 26 Kyungheedae-ro, Dongdaemun-gu, Seoul 02447, Republic of Korea

ARTICLE INFO

Keywords:
Silver nanoparticles
Senna alata extract
Green synthesis
Antimicrobial activity
Potassium ion leakage

ABSTRACT

Biological synthesis of nanomaterials has been increasingly gaining popularity due to its eco-friendly nature and cost-effectiveness. This study aimed to synthesize silver nanoparticles (AgNPs) using *Senna alata* bark extract as reducing and capping agents, and to evaluate their antimicrobial activities. AgNPs was characterized using UV-vis spectrophotometry, transmission electron microscopy, and Fourier transform infrared spectroscopy (FTIR). The formation of AgNPs was monitored by recording the surface plasmon resonance peak observed at 425 nm. High-resolution TEM images elucidated the formation of spherical AgNPs with an average diameter of 10–30 nm. Energy dispersive spectroscopy (EDS) revealed the presence of silver. The functional groups of biomolecules present in the extract and their interaction with AgNPs were identified through FTIR analysis. Biosynthesized AgNPs displayed antimicrobial activity against different microorganisms, including Gram-positive and Gram-negative bacteria as well as fungi, as indicated by the diameter of inhibition zones between 11.37 and 14.87 mm. Minimum inhibitory concentration of AgNPs for the tested microorganisms was in the range from 31.25 to 125 μg/mL. Potassium leakage is a primary indicator of membrane damage which is a significant mode of action of AgNPs against the tested microorganisms. The amount of potassium ions leaked from the microbial cells after 4 h contact time ranged between 0.97 and 3.05 ppm. Morphological changes were observed in all AgNPs-treated microorganisms. The green synthesized AgNPs with high antimicrobial activity has potential to be used in food packaging and biomedical research areas.

1. Introduction

Owing to the outbreak of infectious diseases caused by different types of microorganisms and the development of antibiotic resistance, pharmaceutical companies are searching for new antibacterial agents. Antibacterial applications of nanotechnology are gaining importance to prevent unpredictable consequences of antibiotic resistance. Metal and metal oxide nanoparticles are increasingly used to target bacteria as an alternative to antibiotics. Integration of biosynthesis and nanotechnology has opened new aspects to fight and prevent infections using atomic scale tailoring of materials (Rai et al., 2016).

A fascinating area of nanoparticle research is the formation of unique composite materials with tunable size-dependent properties. Different types of metal nanomaterials such as gold, platinum, copper, and silver have been explored, but silver nanoparticles (AgNPs) has proven to be the most effective as it has good antimicrobial efficacy (Niska et al., 2018). Silver nanoparticles play a significant role in the field of biology and medicine due to its attractive physiochemical properties (Borase et al., 2014; Mittal et al., 2014). Silver nanoparticles can be exploited in medicine for wound healing (Pannerselvam et al., 2017; Shankar et al., 2015), endodontic treatment (Takamiya et al., 2016), treatment of infections in burns (Jadhav et al., 2016), and medical devices (Nandi et al., 2018; Savery et al., 2017).

Biological synthesis has paved way for the greener synthesis of nanoparticles and these have drawn attention as a simple, rapid, stable, cost-effective, and environmental friendly alternative to chemical

* Corresponding author.
** Correspondence to: S P Voravuthikunchai, Natural Product Research Center of Excellence, Prince of Songkla University, Hat Yai, Songkhla 90112, Thailand.
E-mail addresses: shivbiotech@gmail.com (S. Shankar), supayang.v@psu.ac.th (S.P. Voravuthikunchai).

https://doi.org/10.1016/j.mimet.2019.105692
Received 8 July 2019; Received in revised form 14 August 2019; Accepted 16 August 2019
Available online 19 August 2019

procedures and physical methods (Shankar et al., 2014; Singh et al., 2016). Several plants have been successfully used for efficient and rapid extracellular synthesis of AgNPs. Leaf extracts of *Azadirachta indica* (Ahmed et al., 2016), *Atrocarpus altilis* (Ravichandran et al., 2016), *Mussaenda glabrata* (Francis et al., 2017), and many species from Myrtaceae family (Paosen et al., 2017; Shankar et al., 2017) have been successfully synthesized and capped AgNPs with antimicrobial activity.

Senna alata is a native plant in Southeast Asia, Africa, Northern Australia, and Central America (Hennebelle et al., 2009), belongs to the family Fabaceae. It has been demonstrated its potential activity against fungi (Timothy et al., 2012), in contrast, its activity against bacteria remains ambiguous with MIC range of 128–2500 μg/mL (Chomnawang et al., 2009; Rahman, 2004; Wikaningtyas and Sukandar, 2016). It has been used traditionally in herbal medicine for the treatment of conditions such as skin diseases (Hennebelle et al., 2009), pityriasis versicolor (Damodaran and Venkataraman, 1994), and hymenolepisdiminuta (Kundu et al., 2012).

The present study aims to enhance antimicrobial activity of *Senna alata* bark extract by synthesis of AgNPs. The synthesized AgNPs was characterized by UV-visible spectroscopy, transmission electron microscopy, energy dispersive X-ray spectroscopy, zeta potential, Fourier transform infrared spectroscopy, and scanning electron microscopy. The antimicrobial activity and mechanisms of action were assessed.

2. Materials and methods

2.1. Preparation of bark extract and biosynthesis of silver nanoparticles

Bark of *Senna alata* was collected from Hat Yai, Southern Thailand. The plant sample was cleaned and dried in an oven at 60 °C for 48 h and grounded in an electric blender. The plant powder was then extracted with distilled water at 25 °C for 7 days (1:10 (*w/v*) (Saising et al., 2008). The crude extract was concentrated using a rotary evaporator and maintained at 4 °C. For the biosynthesis of AgNPs, the mixture was prepared by adding 0.1 mL of 0.1 M $AgNO_3$ (Merck, St. Louis, MO, USA) solution to 9.8 mL of sterile distilled water containing 0.1 mL of the extracts (50 mg/mL) on a rotary shaker (150 rpm) at 60 °C for 3, 6, 9, and 12 h under dark conditions. Upon completion of the reaction, the samples were centrifuged at 20,000 rpm (Beckman Coulter, California, USA) at 4 °C for 15 min and the pellet was washed twice with distilled water and resuspended in sterile distilled water.

2.2. Characterization of biosynthesized silver nanoparticles

The formation of AgNPs was monitored by UV-visible spectroscopy (Perkins Elmer, Massachusetts, USA) operated at a resolution of 1 nm from 300 to 800 nm. The functional groups present on the AgNPs were recorded using Fourier transform infrared spectroscopy (Bruker, Karlsruhe, Germany) in the range of 500–4000 cm^{-1} with a resolution of 4 cm^{-1}. Shape and size of AgNPs were determined by transmission electron microscopy (JEOL, Massachusetts,USA). Zeta potential was measured by phase analysis light scattering using a ZetaPALS Potential Analyzer (Brookhaven ZetaPlus, New York, USA). The chemical compositions of the particles were analyzed with energy dispersive analysis of X-ray spectroscopy coupled to the scanning electron microscope (Philips X'Pert MPD, Amsterdam, Netherlands).

2.3. Microorganisms and culture conditions

Staphylococcus aureus ATCC 25923, *Acinetobacter baumannii* ATCC 19606, *Escherichia coli* ATCC 25922, *Escherichia coli* O157:H7, *Klebsiella pneumoniae* ATCC 700603, and *Pseudomonas aeruginosa* ATCC 10145 were grown on tryptic soy agar (Difco, Le Pont de Claix, France) at 37 °C for 24 H. *candida albicans* ATCC 90028 was cultured onto Sabouraud dextrose agar (Difco, Le Pont de Claix, France) and incubated at 37 °C overnight. All microorganisms were stored in TSB/SDB containing 20% glycerol at −80 °C until use.

2.4. Antimicrobial activity of biosynthesized silver nanoparticles

2.4.1. Agar well diffusion method

Agar well diffusion method was followed to determine the antimicrobial activity. Briefly, Mueller Hinton agar (Difco, Le Pont de Claix, France) and Sabouraud dextrose agar plates were swabbed with broth culture of respective bacteria and fungi under aseptic conditions. Wells of 6 mm in diameter were filled with 100 μL of the test samples (500 μg/mL) and the plates were allowed to stand for 2 h at 25 °C. Finally, the plates were incubated at 37 °C for 24 h and resulting zone of inhibition diameters were measured. The experiments were performed in triplicate and data were calculated as means ± SD.

2.4.2. Broth microdilution method

Minimum inhibitory concentration (MIC) and minimum bactericidal/fungicidal concentration (MBC/MFC) were determined by broth microdilution method in accordance with Clinical and Laboratory Standardization Institute (CLSI) guideline. Silver nanoparticles were diluted to final concentrations ranging from 250 to 1.95 μg/mL. A 100 μL of diluted bacterial/fungus suspension (10^6 CFU/mL) was added into each well and incubated at 37 °C for 18 h. The MBC and MFC were defined as the lowest concentration of the extract completely preventing bacterial and fungal growth, respectively. All the experiments were carried out in triplicate.

2.5. Measurement of potassium

Potassium leakage was monitored by inductively coupled plasma spectrometry (ICP) using an Optima 8000 (Perkin Elmer, Massachusetts,USA). Microorganisms (2×10^8 cells/mL) were incubated with either 1 × MIC or 2 × MIC of AgNPs for 0.5, 1, 2, and 4 h at 37 °C. The incubated cells were centrifuged at 8000 rpm for 10 min to remove the cell debris. Concentration of potassium ion in the supernatant was expressed as a percentage of the total free potassium ion concentration.

2.6. Scanning electron microscopy

To determine the morphological changes of microorganisms treated with silver nanoparticles, microorganisms (2×10^8 cells/mL) were incubated with 2 × MIC of AgNPs for 4 h at 37 °C and then centrifuged at 3500 rpm for 5 min. The cells were washed three times with 0.1 M PBS (pH 7.4) and fixed in 2.5% (*v*/v) glutaraldehyde for 2 h at 25 °C. The cells were successively dehydrated using 50, 70, 80, 90, and 100% ethanol for 30 min each. After dehydration, the specimens were dried and sputter-coated with gold. Finally, the morphology of the bacterial cells was examined under a SEM (Quanta 400 FEI, Oregon, USA).

2.7. Statistical analysis

Data are presented as means ± standard deviation ($n = 3$). The Student's *t*-test was used to evaluate the significant differences ($p < .05$) between the means.

3. Results and discussion

3.1. Characterization of silver nanoparticles

The formation of silver nanoparticles (AgNPs) by reduction of aqueous silver ions during exposure to the water extract of *Senna alata* bark exhibited reddish-brown colour. The surface plasmon resonance band of AgNPs has been reported in the range of 350–500 nm (Ider et al., 2017). Fig. 1 represents the UV-vis spectra recorded from the reaction medium after heating the solution at 60 °C for 3, 6, 9, and 12 h.

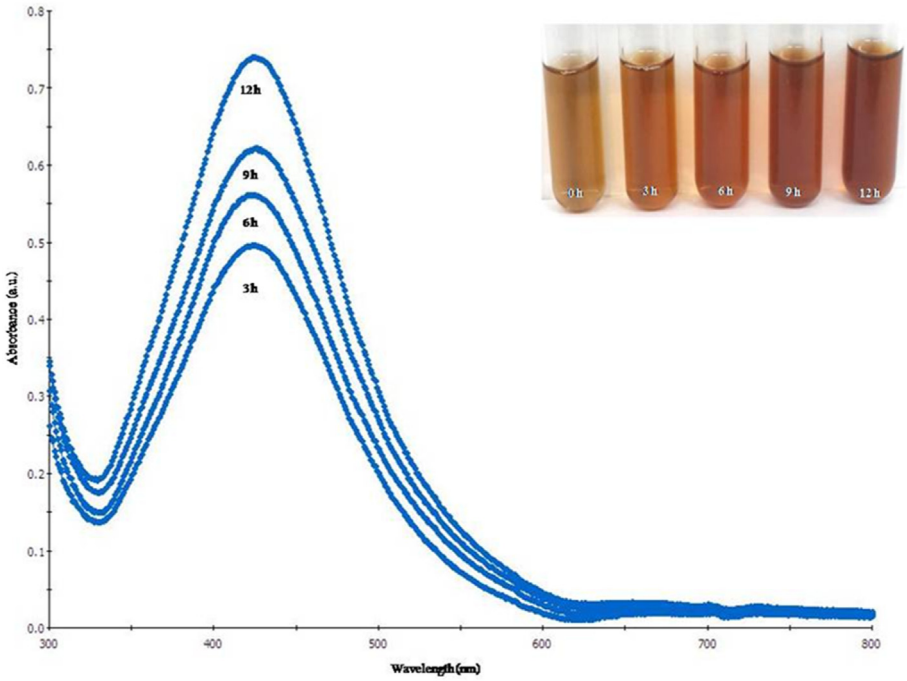

Fig. 1. Time-dependent UV–visible absorption spectra of silver nanoparticles.

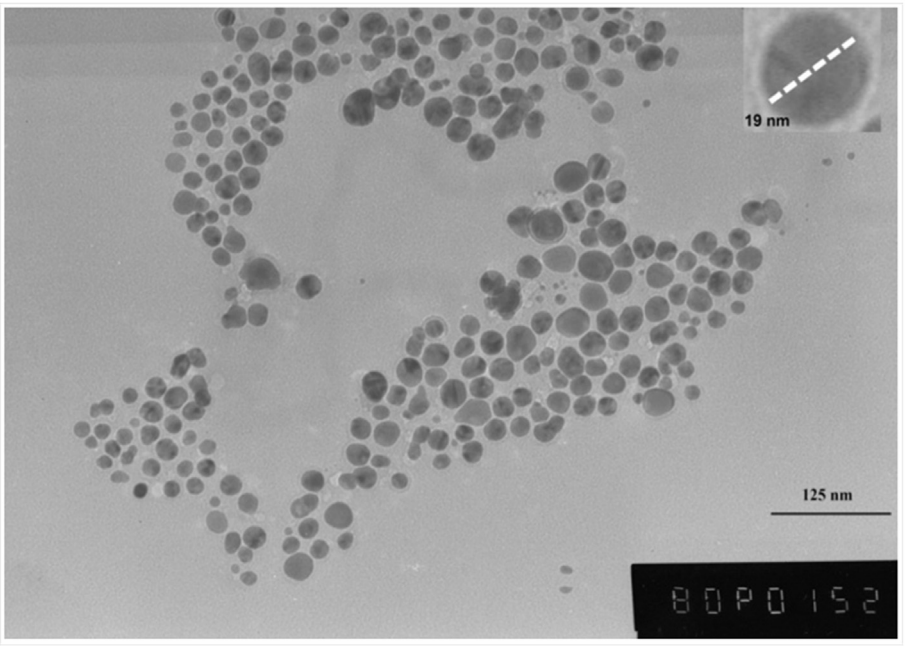

Fig. 2. Tranmission electron micrograph of monodisperse silver nanoparticles.

It was clear that surface plasmon resonance band of AgNPs at 425 nm started appearing from 3 h and become very prominent after 12 h. This clearly demonstrates that the plant extract was able to reduce the silver ions to form AgNPs. Transmission electron microscopy analysis was employed to monitor size, shape, and morphology of biosynthesized AgNPs (Fig. 2). The TEM micrographs elucidated the formation of monodisperse and spherical nanoparticles, which was in agreement with the shape from surface plasmon vibrations band in the UV-vis spectra. Silver nanoparticles had an average diameter between 10 and 30 nm. Some larger particles were observed in the micrographs, might be due to the aggregation of two or more AgNPs. The biosynthesized colloidal AgNPs had a zeta potential of -18.76 ± 1.21 mV, indicating that the surface of the AgNPs was negatively charged and stable in the aqueous solution (Salvioni et al., 2017). This gives further evidence that the AgNPs were capped by bio-molecules from the extract (Rajeshkumar and Bharath, 2017).

Fourier transform infrared spectroscopy (FTIR) analysis was performed to identify the phytochemicals of the plant extracts responsible for the synthesis and stabilization of AgNPs (Fig. 3). The FTIR spectra of the plant extract (Fig. 3a) exhibited absorption bands at 3273 and 2925 cm^{-1}, representing O—H and C—H stretching. The absorption peak located around 1590 cm^{-1} represents NH bending. The presence of the bands at 1449 and 1396 cm^{-1} was related to C—H bond stretching. The band at 1070 cm^{-1} was ascribed to C—O stretching

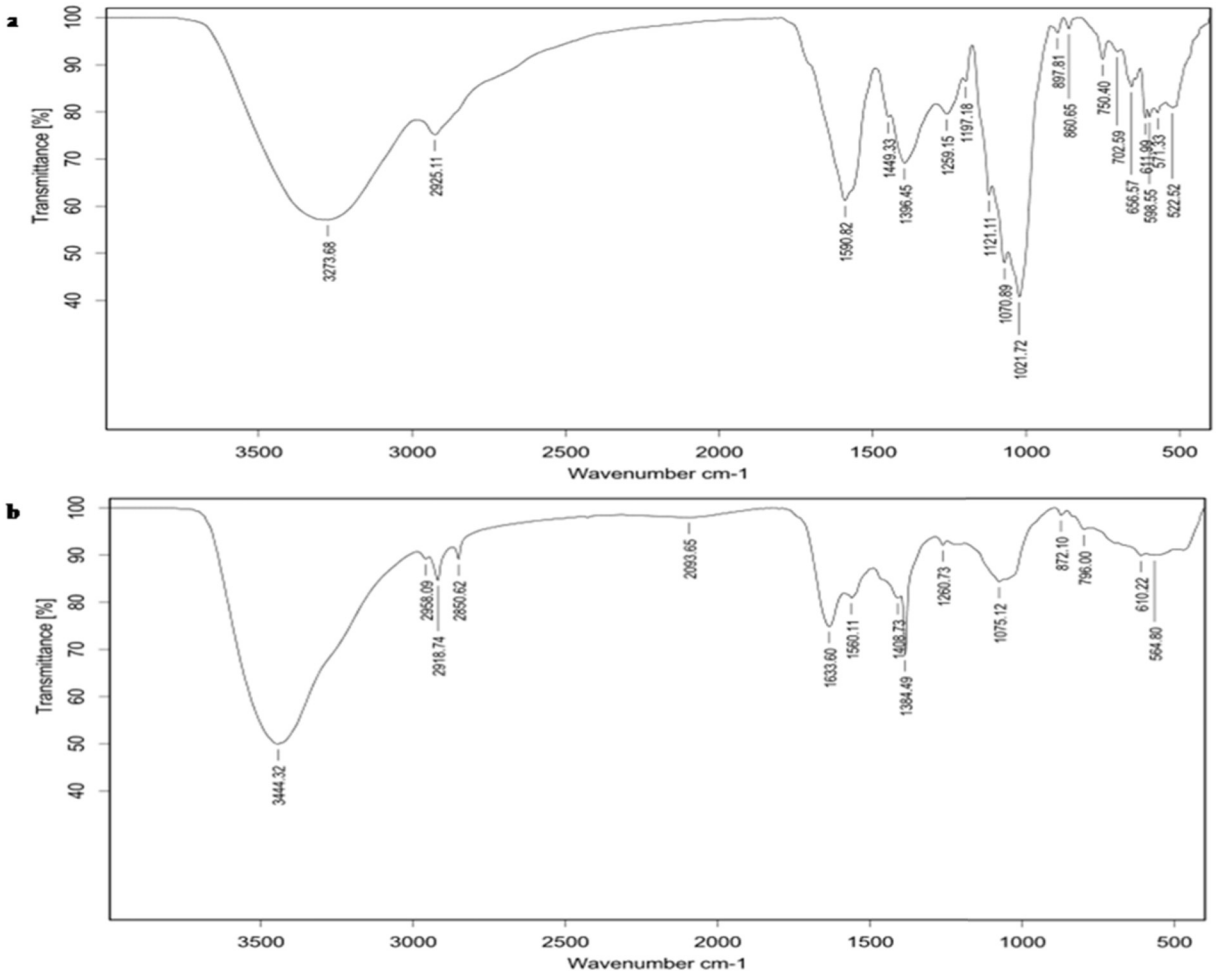

Fig. 3. Fourier transform infrared spectra of (a) *Senna alata* bark extract and (b) silver nanoparticles.

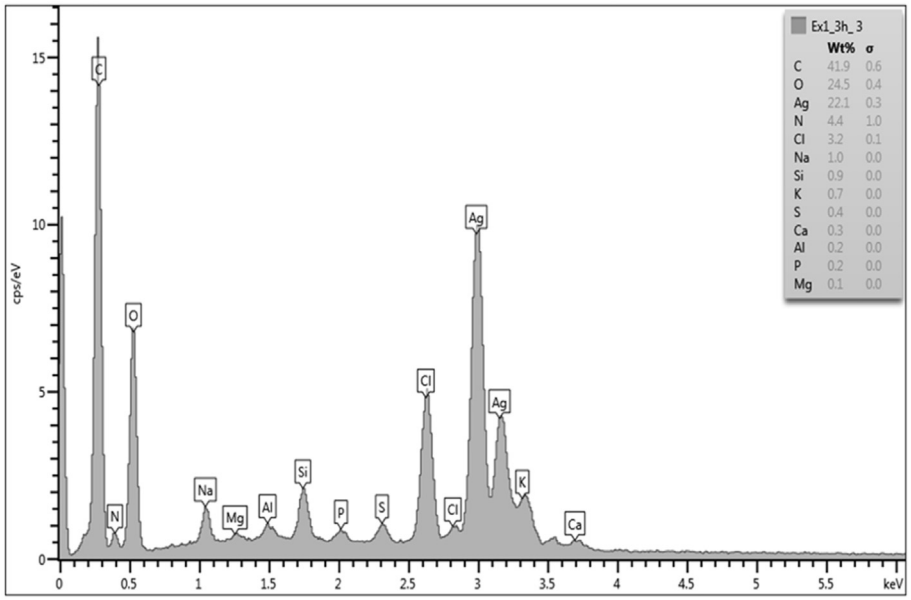

Fig. 4. Energy dispersive analysis of X-ray spectroscopy showing elemental composition of silver nanoparticles.

vibrations of carboxylic acid group. The peak at about 611 cm^{-1} was assigned to aromatic class. After the synthesis of AgNPs (Fig. 3b), these peaks were shifted to 3444, 2918, 1633, 1408, 1384, 1075, and 610 cm^{-1}. All vibration peaks were due to the presence of various alkaloids, anthraquinones, carbohydrates, flavonoids, saponins, tannins, terpenes, steroids and other phytochemicals in the extracts (Abubakar et al., 2015; Sule et al., 2011), that could act as an effective reducing agents. Generally, the phytochemicals donate electrons to

Table 1
Antimicrobial activity of silver nanoparticles synthesized from *Senna alata* bark extract against tested microorganisms.

Microorganisms	Zone of inhibition (mm) by µg/well compounds							MIC/MBC or MFC (µg/mL)		
	CAE (50 µg)	AgNPs (50 µg)	Am B (10 µg)	CAZ (10 µg)	CL (25 µg)	IPM (10 µg)	VA (30 µg)	AgNPs	Antibiotic	CAE
S. aureus	–	14.12 ± 3.00	NA	NA	NA	NA	24.37 ± 0.17	125/ > 250	$0.5/1^{VA}$	> 500
A.baumannii	–	14.87 ± 0.17	NA	NA	21.62 ± 0.17	NA	NA	62.5/250	$1/2^{CL}$	> 500
E. coli	–	13.12 ± 1.23	NA	NA	NA	28.62 ± 0.53	NA	125/250	$0.12/0.25^{IMP}$	> 500
E. coli O157:H7	–	13.00 ± 1.76	NA	NA	NA	32.50 ± 0.35	NA	125/250	$0.25/0.25^{IMP}$	> 500
K. pneumoniae	–	12.75 ± 2.12	NA	NA	NA	23.37 ± 1.94	NA	125/250	$0.25/1^{IMP}$	> 500
P. aeruginosa	–	14.87 ± 0.88	NA	30.12 ± 1.94	NA	NA	NA	62.5/125	$4/16^{CAZ}$	> 500
C. albicans	–	11.37 ± 0.17	15.12 ± 0.17	NA	NA	NA	NA	31.25/62.5	$0.03/0.06^{AmB}$	> 500

–; no inhibition zone, NA; not applicable, CAE; *Cassia alata* bark extract, AgNPs; Silver nanoparticles, AmB; Amphotericin B, CAZ; Ceftazidime, CL; Colistin, IPM; Imipenem, VA; Vancomycin, MIC; Minimum inhibitory concentration, MBC; Minimum bactericidal concentration, MFC; Minimum fungicidal concentration, *S. aureus*; *Staphylococcus aureus* ATCC 25923, *A.baumannii*; *Acinetobacter baumannii* ATCC 19606, *E. coli*; *Escherichia coli* ATCC 25922, *K. pneumoniae*; *Klebsiella pneumoniae* ATCC 700603, *P. aeruginosa*; *Pseudomonas aeruginosa* ATCC 10145, *C. albicans*; *Candida albicans* ATCC 90028. Each value is a mean ± standard deviation.

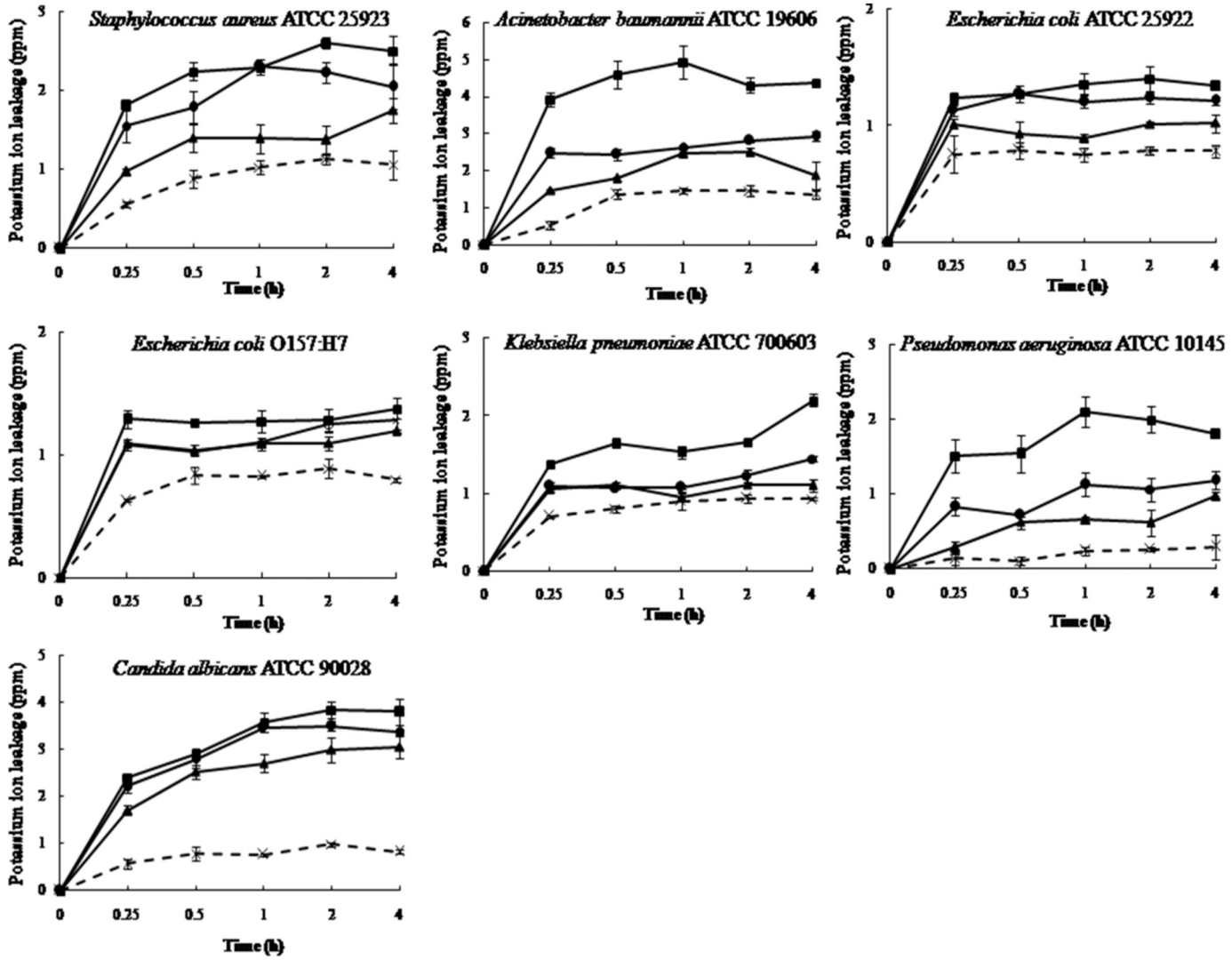

Fig. 5. Effects of silver nanoparticles on potassium ion leakage from tested microorganisms at MIC (▲), 2MIC (●), 0.5% Triton-X (■), and control (x) at different time intervals.

metal ions and reduce them to metallic nanoparticles (Shukla and Iravani, 2017).

Energy dispersive analysis of X-ray spectroscopy (EDX) confirmed the presence of silver in the sample which proved the formation of AgNPs (Fig. 4). It showed that AgNPs were in atomic state, which caused by the reduction of sliver ions. Metallic silver nanocrystals generally showed typical optical absorption peak approximately at 3 keV due to their strong surface plasmon resonance transition (Bindhu and Umadevi, 2014). The spectrum of AgNPs synthesized with the extract demonstrated silver signal at 22.1%. The existence of elemental silver with the signals of carbon and oxygen atoms might be due to the presence of organic compounds in the extract of *Senna alata*, which

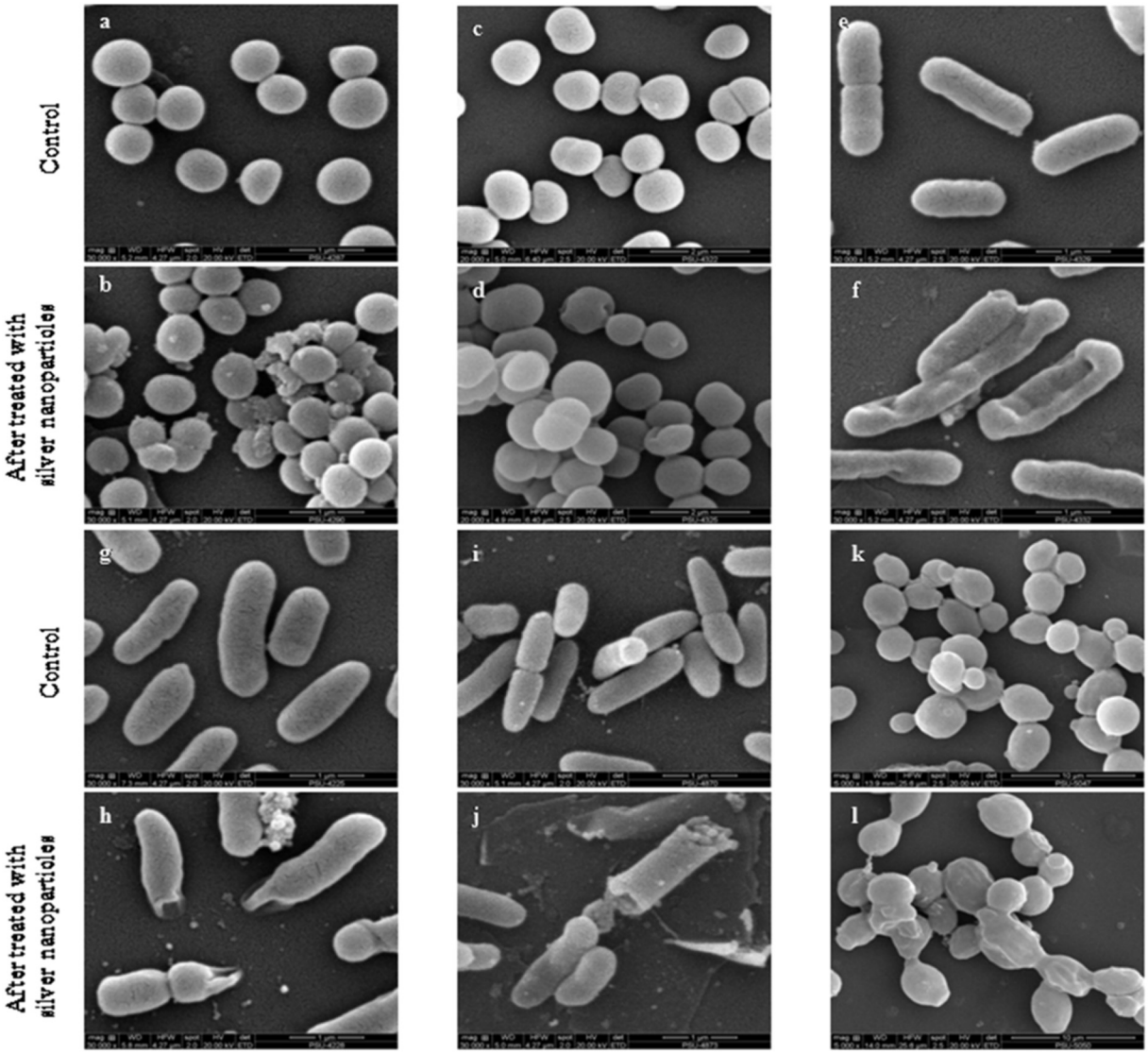

Fig. 6. Scanning electron microscopy study of *Staphylococcus aureus* ATCC 25923 (a), *Acinetobacter baumannii* ATCC 19606 (c), *Escherichia coli* O157:H7 (e), *Klebsiella pneumoniae* ATCC 700603 (g), *Pseudomonas aeruginosa* ATCC 10145 (i), *Candida albicans* ATCC 90028 (k) after exposure to 2 × MIC silver nanoparticles for 4 h. The control (a, c, e, g, and i) was processed without silver nanoparticles, showing a bright and smooth surface. Treated cultures (b, d, f, h, j, and l) which were exposed to the nanoparticles, showing roughened, corrugated, with atrophy and fracture.

capped the AgNPs and stabilized them. In this study, inductively coupled plasma optical emission spectrometer was used to determine the concentration of silver in the prepared AgNPs, resulting in silver concentration of approximately 14.46 ± 0.23 μg/mL.

3.2. Antimicrobial activity of silver nanoparticles

The microorganisms were selected to cover all range of important human pathogenic microorganisms, including Gram-positive, Gram-negative bacteria, and fungi. Silver nanoparticles at 50 μg/well displayed antimicrobial activity against different microorganisms, as indicated by diameter of inhibition zones of 11.37–14.87 mm (Table 1). *Senna alata* bark extract at the same concentration showed no inhibitory activity against all bacteria and yeast strains. Minimum inhibitory concentration of AgNPs for the tested microorganisms was in the range of 31.25–125 μg/mL (Table 1). Bactericidal and fungicidal activity were between 62.25 and 250 μg/mL for almost all the test pathogens, except *Staphylococcus aureus*. AgNPs synthesized with plant belonging to same family (Fabaceae) *Acacia leucophloea* extract (Murugan et al., 2014), *Medicago sativa* (Alfalfa) leaves (Baraka et al., 2017) have been found to possess enhance antimicrobial properties. The actual bactericidal mechanism of AgNPs has not yet been well-established. Antibacterial effects of AgNPs may be due to the different physiological properties of Gram-positive and Gram-negative bacteria. The cell wall of Gram-positive bacteria is composed of a thick peptidoglycan layer consisting of linear polysaccharide chains cross linked by short peptides, thus forming more rigid structure making it difficult for AgNPs either to attach to the cell wall or penetrate (Arokiyaraj et al., 2014). Gram-negative bacteria have a cytoplasmic membrane, a thin peptidoglycan layer, and an outer membrane containing lipopolysaccharide. It has been reported that positive charge on silver ions bind to the negatively charged bacterial cell wall (Franci et al., 2015). Some researchers suggested that silver ions reacted with DNA, resulting in DNA fragmentation (Jiravova et al., 2016). In author context, AgNPs react with multiple enzymes, transporter proteins, and nucleic, leading to the cell death (Gomaa, 2017). Silver nanoparticles exhibitied very strong fungicidal property, which could be specific affinity to membranes of a hypha (Tutaj et al., 2016). In addition, the antimicrobial potency of green synthesized AgNPs has attracted various attention with applications in many areas of research. AgNPs has been used as active agent in

the design of biomedical devices (Burdușel et al., 2018) and food packaging materials (Wu et al., 2018).

3.3. Measurement of potassium ion leakage

Antimicrobial mode of action of AgNPs against the tested microorganisms was confirmed by measuring potassium ion leakage from the treated cells (Fig. 5). When the organisms were exposed to AgNPs suspension for 15 min at MIC, potassium ions leaked from *S. aureus*, *A. baumannii*, *E. coli*, *E. coli* O157:H7, *K. pneumoniae*, *P. aeruginosa*, and *C. albicans* were 0.97, 0.14, 1.01, 1.09, 1.05, 0.28, and 1.70 ppm, respectively. The amount of potassium ions leaked from the microbial cells after 4 h contact time ranged between 0.97 and 3.05 ppm. The same trend of leakage was observed when the concentration of AgNPs was increased to 2MIC. The potassium ion leakage ranging from 0.82–2.25 ppm after 15 min and reached 1.18–3.35 ppm by 4 h. The bacterial plasma membrane constitutes a permeability barrier against small ions like potassium ions, which are necessary electrolytes for proper membrane function and enzyme activity (Bajpai et al., 2016). The internal ionic environment of organisms is generally potassium-rich. This impermeability to small ions is regulated by the structural and chemical composition of the cell membrane. Increase in leakage of potassium ions in microorganisms could be an indication of disruption of this permeability barrier (Akinpelu et al., 2015). Therefore, even relatively slight changes to the structural integrity of cell membranes can detrimentally affect cell metabolism, leading to the cell death (Zhang et al., 2016). In the case of the tested microorganisms, monitoring potassium ions efflux may be a more sensitive indicator of membrane damage.

3.4. Scanning electron microscopy of the microbial treated with silver nanoparticles

Silver nanoparticles dissipate the membrane electrical potential by disrupting the membrane bilayer, resulting in intracellular ion efflux, leakage of the cell contents, and finally cell death (Dosunmu et al., 2015). In this study, microbial morphological changes and membrane integrity upon treatment with AgNPs were observed by SEM (Fig. 6). The results confirmed extensive damage to the cell membrane in the presence of AgNPs (Fig. 6b, d, f, h, j, l), in contrast to the smooth surfaces of the untreated samples (Fig. 6a, c, e, g, i, k). The images illustrated a possible mechanism of action whereby AgNPs interact with the cell membrane, causing membrane permeabilization and degradation, with accompanying changes in cell morphology.

4. Conclusions

The AgNPs was synthesized using *Senna alata* bark extract as a reducing and capping agents. The synthesis of AgNPs was monitored and characterized by UV-visible spectroscopy, EDS, TEM, and FTIR analysis. The AgNPs were uniform in size and spherical in shape. The FTIR results showed the capping of AgNPs with the biomolecules from plant extract. The biosynthesized AgNPs showed potent antimicrobial activity against broad range of Gram-positive and Gram-negative bacteria as well as fungus. The synthesized AgNPs has potential to be useful in variety of antimicrobial applications in the preparation of health care agents for the treatment of human diseases and design of antimicrobial materials such as food packaging films.

Declaration of Competing Interest

The authors report no conflicts of interest.

Acknowledgments

This work was supported by TRF Senior Research Scholar (Grant No. RTA618006), the Thailand Research Fund and Natural Product Research Center of Excellence, Prince of Songkla University.

References

Abubakar, I., Mann, A., Mathew, J.T., 2015. Phytochemical composition, antioxidant and anti-nutritional properties of root-bark and leaf methanol extracts of *Senna alata* L. grown in Nigeria. Afr. J. Pure Appl. Chem. 9, 91–97.
Ahmed, S., Saifullah, Ahmad, M., Swami, B.L., Ikram, S., 2016. Green synthesis of silver nanoparticles using *Azadirachta indica* aqueous leaf extract. J. Radiat. Res. Appl. Sci. 9, 1–7.
Akinpelu, D., Aiyegoro, O., Akinpelu, O., Okoh, A., 2015. Stem bark extract and fraction of *Persea americana* (Mill.) exhibits bactericidal activities against strains of *Bacillus cereus* associated with food poisoning. Molecules 20, 416–429.
Arokiyaraj, S., Arasu, M.V., Vincent, S., Prakash, N.U., Choi, S.H., Oh, Y.-K., Choi, K.C., Kim, K.H., 2014. Rapid green synthesis of silver nanoparticles from *Chrysanthemum indicum* L and its antibacterial and cytotoxic effects: an in vitro study. Int. J. Nanomedicine 9, 379.
Bajpai, V.K., Singh, S., Mehta, A., 2016. Chemical characterization and mode of action of *Ligustrum lucidum* flower essential oil against food-borne pathogenic bacteria. Bangladesh J. Pharmacol 11, 269–280.
Baraka, A., Dickson, S., Gobara, M., El-Sayyad, G.S., Zorainy, M., Awaad, M.I., Hatem, H., Kotb, M.M., Tawfic, A., 2017. Synthesis of silver nanoparticles using natural pigments extracted from Alfalfa leaves and its use for antimicrobial activity. Chem. Pap. 71, 2271–2281.
Bindhu, M.R., Umadevi, M., 2014. Surface plasmon resonance optical sensor and antibacterial activities of biosynthesized silver nanoparticles. Spectrochim. Acta A Mol. Biomol. Spectrosc. 121, 596–604.
Borase, H.P., Salunke, B.K., Salunkhe, R.B., Patil, C.D., Hallsworth, J.E., Kim, B.S., Patil, S.V., 2014. Plant extract: a promising biomatrix for ecofriendly, controlled synthesis of silver nanoparticles. Appl. Biochem. Biotechnol. 173, 1–29.
Burdușel, A.C., Gherasim, O., Grumezescu, A., Mogoantă, L., Ficai, A., Andronescu, E., 2018. Biomedical applications of silver nanoparticles: an up-to-date overview. Nanomaterials 8, 681.
Chomnawang, M.T., Surassmo, S., Wongsariya, K., Bunyapraphatsara, N., 2009. Antibacterial activity of Thai medicinal plants against methicillin-resistant *Staphylococcus aureus*. Fitoterapia 80, 102–104.
Damodaran, S., Venkataraman, S., 1994. A study on the therapeutic efficacy of *Cassia alata*, Linn. leaf extract against *Pityriasis versicolor*. J. Ethnopharmacol. 42, 19–23.
Dosunmu, E., Chaudhari, A.A., Singh, S.R., Dennis, V.A., Pillai, S.R., 2015. Silver-coated carbon nanotubes downregulate the expression of *Pseudomonas aeruginosa* virulence genes: a potential mechanism for their antimicrobial effect. Int. J. Nanomedicine 10, 5025.
Franci, G., Falanga, A., Galdiero, S., Palomba, L., Rai, M., Morelli, G., Galdiero, M., 2015. Silver nanoparticles as potential antibacterial agents. Molecules 20, 8856–8874.
Francis, S., Joseph, S., Koshy, E.P., Mathew, B., 2017. Green synthesis and characterization of gold and silver nanoparticles using *Mussaenda glabrata* leaf extract and their environmental applications to dye degradation. Environ. Sci. Pollut. Res. 24, 17347–17357.
Gomaa, E.Z., 2017. Silver nanoparticles as an antimicrobial agent: a case study on *Staphylococcus aureus* and *Escherichia coli* as models for gram-positive and gram-negative bacteria. J. Gen. Appl. Microbiol. 63, 36–43.
Hennebelle, T., Weniger, B., Joseph, H., Sahpaz, S., Bailleul, F., 2009. Senna alata. Fitoterapia 80, 385–393.
Ider, M., Abderrafi, K., Eddahbi, A., Ouaskit, S., Kassiba, A., 2017. Silver metallic nanoparticles with surface plasmon resonance: synthesis and characterizations. J. Clust. Sci. 28, 1051–1069.
Jadhav, K., Dhamecha, D., Bhattacharya, D., Patil, M., 2016. Green and ecofriendly synthesis of silver nanoparticles: characterization, biocompatibility studies and gel formulation for treatment of infections in burns. J. Photochem. Photobiol. B Biol. 155, 109–115.
Jiravova, J., Tomankova, K.B., Harvanova, M., Malina, L., Malohlava, J., Luhova, L., Panacek, A., Manisova, B., Kolarova, H., 2016. The effect of silver nanoparticles and silver ions on mammalian and plant cells *in vitro*. Food Chem. Toxicol. 96, 50–61.
Kundu, S., Roy, S., Lyndem, L.M., 2012. Cassia alata L: potential role as anthelmintic agent against *Hymenolepis diminuta*. Parasitol. Res. 111, 1187–1192.
Mittal, A.K., Bhaumik, J., Kumar, S., Banerjee, U.C., 2014. Biosynthesis of silver nanoparticles: elucidation of prospective mechanism and therapeutic potential. J. Colloid Interface Sci. 415, 39–47.
Murugan, K., Senthilkumar, B., Senbagam, D., Al-Sohaibani, S., 2014. Biosynthesis of silver nanoparticles using Acacia leucophloea extract and their antibacterial activity. Int. J. Nanomedicine 9, 2431.
Nandi, S.K., Shivaram, A., Bose, S., Bandyopadhyay, A., 2018. Silver nanoparticle deposited implants to treat osteomyelitis. J Biomed Mater Res B Appl Biomater 106, 1073–1083.
Niska, K., Zielinska, E., Radomski, M.W., Inkielewicz-Stepniak, I., 2018. Metal nanoparticles in dermatology and cosmetology: interactions with human skin cells. Chem. Biol. Interact. 295, 38–51.
Pannerselvam, B., Jothinathan, M.K.D., Rajenderan, M., Perumal, P., Thangavelu, K.P., Kim, H.J., Singh, V., Rangarajulu, S.K., 2017. An in vitro study on the burn wound healing activity of cotton fabrics incorporated with phytosynthesized silver nanoparticles in male Wistar albino rats. Eur. J. Pharm. Sci. 100, 187–196.
Paosen, S., Saising, J., Septama, A.W., Voravuthikunchai, S.P., 2017. Green synthesis of silver nanoparticles using plants from Myrtaceae family and characterization of their

antibacterial activity. Mater. Lett. 209, 201–206.
Rahman, Ì., 2004. Brine shrimp toxicity of leaf and seed extracts of *Cassia alata* Linn, and their antibacterial potency. J. Med. Sci. 4, 188–193.
Rai, M., Ingle, A.P., Birla, S., Yadav, A., Santos, C.A.D., 2016. Strategic role of selected noble metal nanoparticles in medicine. Crit. Rev. Microbiol. 42, 696–719.
Rajeshkumar, S., Bharath, L., 2017. Mechanism of plant-mediated synthesis of silver nanoparticles–a review on biomolecules involved, characterisation and antibacterial activity. Chem. Biol. Interact. 273, 219–227.
Ravichandran, V., Vasanthi, S., Shalini, S., Shah, S.A.A., Harish, R., 2016. Green synthesis of silver nanoparticles using *Atrocarpus altilis* leaf extract and the study of their antimicrobial and antioxidant activity. Mater. Lett. 180, 264–267.
Saising, J., Hiranrat, A., Mahabusarakam, W., Ongsakul, M., Voravuthikunchai, S.P., 2008. Rhodomyrtone from Rhodomyrtus tomentosa (Aiton) Hassk. as a natural antibiotic for staphylococcal cutaneous infections. J. Health Sci. 54, 589–595.
Salvioni, L., Galbiati, E., Collico, V., Alessio, G., Avvakumova, S., Corsi, F., Tortora, P., Prosperi, D., Colombo, M., 2017. Negatively charged silver nanoparticles with potent antibacterial activity and reduced toxicity for pharmaceutical preparations. Int. J. Nanomedicine 12, 2517.
Savery, L.C., Viñas, R., Nagy, A.M., Pradeep, P., Merrill, S.J., Hood, A.M., Malghan, S.G., Goering, P.L., Brown, R.P., 2017. Deriving a provisional tolerable intake for intravenous exposure to silver nanoparticles released from medical devices. Regul. Toxicol. Pharmacol. 85, 108–118.
Shankar, S., Jaiswal, L., Aparna, R.S.L., Prasad, R.G.S.V., 2014. Synthesis, characterization, *in vitro* biocompatibility, and antimicrobial activity of gold, silver and gold silver alloy nanoparticles prepared from *Lansium domesticum* fruit peel extract. Mater. Lett. 137, 75–78.
Shankar, S., Jaiswal, L., Aparna, R.S.L., Prasad, R.G.S.V., Kumar, G.P., Manohara, C.M., 2015. Wound healing potential of green synthesized silver nanoparticles prepared from *Lansium domesticum* fruit peel extract. Mater. Express 5, 159–164.
Shankar, S., Leejae, S., Jaiswal, L., Voravuthikunchai, S.P., 2017. Metallic nanoparticles augmented the antibacterial potency of Rhodomyrtus tomentosa acetone extract against *Escherichia coli*. Microb. Pathog. 107, 181–184.
Shukla, A.K., Iravani, S., 2017. Metallic nanoparticles: green synthesis and spectroscopic characterization. Environ. Chem. Lett. 15, 223–231.
Singh, P., Kim, Y.-J., Zhang, D., Yang, D.-C., 2016. Biological synthesis of nanoparticles from plants and microorganisms. Trends Biotechnol. 34, 588–599.
Sule, W.F., Okonko, I.O., Omo-Ogun, S., Nwanze, J.C., Ojezele, M.O., Ojezele, O.J., Alli, J.A., Soyemi, E.T., Olaonipekun, T.O., 2011. Phytochemical properties and in-vitro antifungal activity of *Senna alata* Linn. crude stem bark extract. J. Med. Plant Res. 5, 176–183.
Takamiya, A.S., Monteiro, D.R., Bernabé, D.G., Gorup, L.F., Camargo, E.R., Gomes-Filho, J.E., Oliveira, S.H.P., Barbosa, D.B., 2016. *In vitro* and *in vivo* toxicity evaluation of colloidal silver nanoparticles used in endodontic treatments. J. Endod. 42, 953–960.
Timothy, S.Y., Wazis, C.H., Adati, R.G., Maspalma, I.D., 2012. Antifungal activity of aqueous and ethanolic leaf extracts of *Cassia alata* Linn. J. Appl. Pharma. Sci 2, 182.
Tutaj, K., Szlazak, R., Szalapata, K., Starzyk, J., Luchowski, R., Grudzinski, W., Osinska-Jaroszuk, M., Jarosz-Wilkolazka, A., Szuster-Ciesielska, A., Gruszecki, W.I., 2016. Amphotericin B-silver hybrid nanoparticles: synthesis, properties and antifungal activity. Nanomedicine 12, 1095–1103.
Wikaningtyas, P., Sukandar, E.Y., 2016. The antibacterial activity of selected plants towards resistant bacteria isolated from clinical specimens. Asian Pac. J. Trop. Biomed. 6, 16–19.
Wu, Z., Huang, X., Li, Y.-C., Xiao, H., Wang, X., 2018. Novel chitosan films with laponite immobilized Ag nanoparticles for active food packaging. Carbohydr. Polym. 199, 210–218.
Zhang, Y., Liu, X., Wang, Y., Jiang, P., Quek, S., 2016. Antibacterial activity and mechanism of cinnamon essential oil against Escherichia coli and Staphylococcus aureus. Food Control 59, 282–289.